

# SPARK PLASMA SINTERING OF $\beta$ -SiAlON–BN COMPOSITES

## СПАРК-ПЛАЗМЕННОЕ СПЕКАНИЕ КОМПОЗИТОВ НА ОСНОВЕ $\beta$ -SiAlON–BN

Nefedova E.<sup>1</sup>, Ph.D. Grigoryev E.<sup>1</sup>, Fokin D.<sup>1</sup>, Ph.D. Smirnov K.<sup>2</sup>

<sup>1</sup> National Research Nuclear University MEPhI - Moscow, Russia

<sup>2</sup> Institute of Structural Macrokinetics and Materials Science, Russian Academy of Sciences - Moscow, Russia

**Abstract:** Investigated was the spark plasma sintering (SPS) of  $\beta$ -SiAlON/0–30 wt % BN ceramic composites. The raw materials ( $\beta$ -Si<sub>5</sub>AlON<sub>7</sub> and BN powders) were prepared by infiltration-mediated combustion synthesis (CS). Experimentally established were the following process parameters for SPS of composites with high relative density (>95 %) and flexural strength of 250–300 MPa: (a) heating rate 50 deg/min, (b) maximum temperature 1650–1750°C, (c) and holding time 5 min.

**KEYWORDS:** COMBUSTION SYNTHESIS, SPARK PLASMA SINTERING, CERAMIC COMPOSITES, SIALONS, BORON NITRIDE

### 1. Introduction

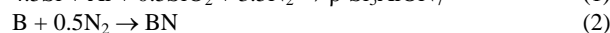
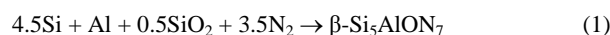
Solid solutions of  $\beta$ -Si<sub>3</sub>N<sub>4</sub> of general formula Si<sub>6- $\zeta$</sub> Al <sub>$\zeta$</sub> O <sub>$\zeta$</sub> N<sub>8- $\zeta$</sub>  ( $\zeta = 0.0$ – $4.2$ ) are known for their excellent hardness, strength, and wear/corrosion resistance, which explains their wide use in various engineering applications such as refractory materials, in bearings, and in cutting instruments [1]. On the other hand, ceramics containing hexagonal BN (h-BN) exhibit good electroinsulating properties combined with high thermal conductivity and corrosion resistance at exceeding low wettability with melts of different metals and non-metals [2]. Addition of h-BN to ceramic composites is known to improve their thermal shock resistance, machinability, and tribological properties [3–5]. BN-containing composites,  $\beta$ -Si<sub>6- $\zeta$</sub> Al <sub>$\zeta$</sub> O <sub>$\zeta$</sub> N<sub>8- $\zeta$</sub> -BN, are highly promising for metallurgical applications such as tubes for metal pouring, pipe heaters, nozzles, dozer units, annular breakers, buckets, crucibles, lining plates, thermocouple casing, sensor level gages, etc.

Combustion synthesis (CS) is a convenient technique for production of SIALON powders with desired composition, particle size, and morphology [6–8]. Spark plasma sintering (SPS) is a newly developed process that allows pulsed direct current to pass through the die and sample to heat them. Compared with conventional hot pressing, SPS allows higher heating rates and a very short holding time. SPS has been widely proven as a rapid and effective densification method for various materials [9, 10].

In this context, it seemed interesting to apply the combination of these advanced techniques to fabrication of high-density  $\beta$ -SiAlON–BN ceramic composites with improved functional properties.

### 2. Experimental procedure

Infiltration-mediated SHS of  $\beta$ -Si<sub>5</sub>AlON<sub>7</sub> and BN powders in nitrogen gas was carried out by the following schemes:



Green mixtures also contained some amount of diluents,  $\beta$ -Si<sub>5</sub>AlON<sub>7</sub> and h-BN respectively, in order to improve extent of conversion. Commercial powders of Si (mean particle size  $d < 10 \mu\text{m}$ ), Al ( $d = 20$ – $50 \mu\text{m}$ ), SiO<sub>2</sub> ( $d < 10 \mu\text{m}$ ), B ( $d = 1 \mu\text{m}$ ), and home-made powders of  $\beta$ -Si<sub>5</sub>AlON<sub>7</sub> ( $d \sim 5 \mu\text{m}$ ) and h-BN ( $d \sim 2 \mu\text{m}$ ) were used in our experiments. Aliquot amounts of the above powders were dry milled for 1–2 h in a mill with Si<sub>3</sub>N<sub>4</sub> milling balls. Combustion was performed in a 2-L vessel at  $P(\text{N}_2) = 8$ – $10 \text{ MPa}$ .

Mixtures of combustion-synthesized  $\beta$ -Si<sub>5</sub>AlON<sub>7</sub> and h-BN powders also containing 0–8 wt % commercial Y<sub>2</sub>O<sub>3</sub> powder as a sintering aid were intermixed in a high-energy planetary steel-ball mill. Ball milling time (800 rpm, ball/mill ratio 10 : 1) was 5 min. The milled powders (about 0.5 g) were placed into a graphite die 10.4 mm in inner diameter and sintered in a Labox 625 SPS facility

under vacuum (gas pressure below 10 Pa). The pieces of carbon paper and carbon felt were put between the powder and graphite die to exclude the high temperature reaction during sintering, as well as to easily get the sample out of the graphite die after sintering. The heating rate was 50 deg/min. The sintered compacts were heated from room temperature to 600°C without applied load and then to 1550–1800°C at a compressive stress of 50 MPa. The compacts were held at a desired temperature for 5 min before the power was turned off. Temperature monitoring during sintering between 600°C and final sintering temperature was carried out using an optical pyrometer, focused on a hole on the surface of the carbon die.

The particle size distribution of milled powders was determined with Fritsch Analysette 22 device. The BET was characterized by N<sub>2</sub> sorption using a Sorbi-M surface area analyzer. The raw powders and sintered compacts were characterized by XRD (DRON-3.0) and SEM (JEOL 6610L). Sample densities were determined by hydrostatic weighing. Flexural strength ( $\sigma_f$ ) was measured for bending a thin disk on a ring base in a universal testing machine Instron-5966.

### 3. Results and discussion

According to XRD and SEM results, the raw powders of  $\beta$ -Si<sub>5</sub>AlON<sub>7</sub> and BN did not contain impurity phases and were present largely as agglomerates. Their SEM images are given in Fig. 1. The specific surface ( $s$ ) of as-synthesized  $\beta$ -Si<sub>5</sub>AlON<sub>7</sub> and h-BN powders was 1.3 and 9.8 m<sup>2</sup>/g, respectively.

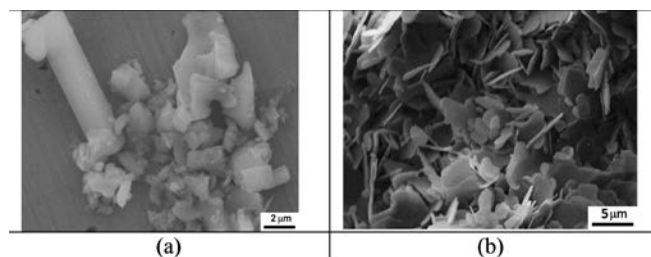


Fig. 1. SEM images of raw  $\beta$ -Si<sub>5</sub>AlON<sub>7</sub> (a) and h-BN (b) powders.

After ball milling, the  $s$  values increased by a factor of 4–6 (Table 1). The size distribution of h-BN-containing mixtures exhibited an additional peak around 20–60  $\mu\text{m}$ , thus indicating the formation of secondary huge agglomerates from initially fine particles.

Table 1.

	Specific surface $s$ (m <sup>2</sup> /g) of as-synthesized and ball-milled powders			
	$\beta$ -Si <sub>5</sub> AlON <sub>7</sub>	$\beta$ -Si <sub>5</sub> AlON <sub>7</sub> /10% BN	$\beta$ -Si <sub>5</sub> AlON <sub>7</sub> /20% BN	$\beta$ -Si <sub>5</sub> AlON <sub>7</sub> /30% BN
As-synthesized	1.27	2.14	2.99	3.85
Ball-milled	4.83	7.62	14.36	22.8

The sintering of undoped  $\beta$ - $\text{Si}_5\text{AlON}_7$  was accompanied (Fig. 2) by marked increase in sample shrinkage around  $1400^\circ\text{C}$  probably due to formation of  $\text{SiO}_2$  and  $\text{Al}_2\text{O}_3$  eutectics. Upon further increase in  $T$ , the relative density of sintered ceramics gradually grows from 75 to 87% (Fig. 3). Our SEM results suggest that at  $T = 1550^\circ\text{C}$  the particles remain practically unchanged and the formation of bottle necks gets started at higher temperatures. According to XRD data, the ceramics sintered above  $1750^\circ\text{C}$  exhibit the presence of  $\text{AlN}$  formed upon thermal decomposition of  $\beta$ - $\text{Si}_5\text{AlON}_7$ . This is also evidenced by some increase in gas pressure in the reactor observed above  $1600^\circ\text{C}$  and caused by the release of gaseous decomposition products,  $\text{N}_2$  and  $\text{SiO}$ . Note that the release of gaseous products was observed only for sintered materials with  $\rho_{\text{rel}} < 87\%$ . In case of denser materials having no open porosity, the decomposition of  $\beta$ - $\text{Si}_5\text{AlON}_7$  was completely suppressed.

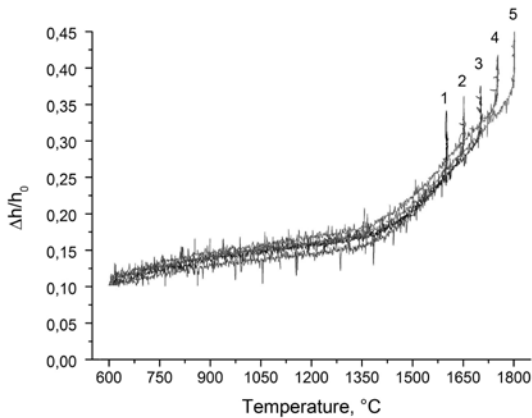


Fig. 2. Linear shrinkage  $\Delta h/h_0$  for  $\beta$ - $\text{Si}_5\text{AlON}_7$  as a function of temperature  $T$  for  $T_{\text{max}} = 1600$  (1),  $1650$  (2),  $1700$  (3),  $1750$  (4), and  $1800^\circ\text{C}$  (5).

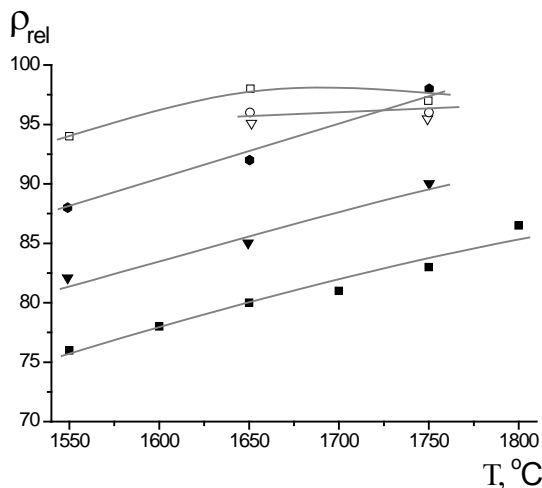


Fig. 3. Relative density  $\rho_{\text{rel}}$  as a function of  $T_{\text{max}}$  for: (■)  $\beta$ - $\text{Si}_5\text{AlON}_7$ , (▼)  $\beta$ - $\text{Si}_5\text{AlON}_7$ - $\text{Y}_2\text{O}_3$  (2.5 wt %), (●)  $\beta$ - $\text{Si}_5\text{AlON}_7$ - $\text{Y}_2\text{O}_3$  (5 wt %), (▽)  $\beta$ - $\text{Si}_5\text{AlON}_7$ -BN (10 wt %), (□)  $\beta$ - $\text{Si}_5\text{AlON}_7$ -BN (20 wt %), (○)  $\beta$ - $\text{Si}_5\text{AlON}_7$ -BN (30 wt %).

Figure 4a shows relative density  $\rho_{\text{rel}}$  as a function of temperature  $T$  for  $\beta$ - $\text{Si}_5\text{AlON}_7$  and  $\beta$ - $\text{Si}_5\text{AlON}_7$ - $\text{Y}_2\text{O}_3$  ceramics. The addition of  $\text{Y}_2\text{O}_3$  is seen to improve the efficiency of sintering for  $T > 1400^\circ\text{C}$ , that is, after the formation of liquid eutectics with oxides. A density close to theoretical can be attained upon addition of 5 wt %  $\text{Y}_2\text{O}_3$  (Fig. 3), which agrees with our previous results [11] on sintering SHS-produced  $\beta$ - $\text{SiAlON}$  powders in furnace under pressure of nitrogen gas.

The addition of h-BN also facilitates SPS but by another mechanism: h-BN improves the compactibility of sintered powder mixtures. Under a compressive stress of 50 MPa at  $600^\circ\text{C}$ , the initial value of  $\rho_{\text{rel}}$  exceeds 0.80 for the compact containing 30 wt % h-BN, and 0.6 for that of undoped  $\beta$ - $\text{Si}_5\text{AlON}_7$  (Fig. 4b). In parallel,

an increase in h-BN content suppresses the consolidation processes related to the formation of liquid eutectics. At 30 wt % h-BN (curve 4 in Fig. 4b), an increase in  $\rho_{\text{rel}}$  above  $1400^\circ\text{C}$  becomes insignificant even in the presence of  $\text{Y}_2\text{O}_3$ .

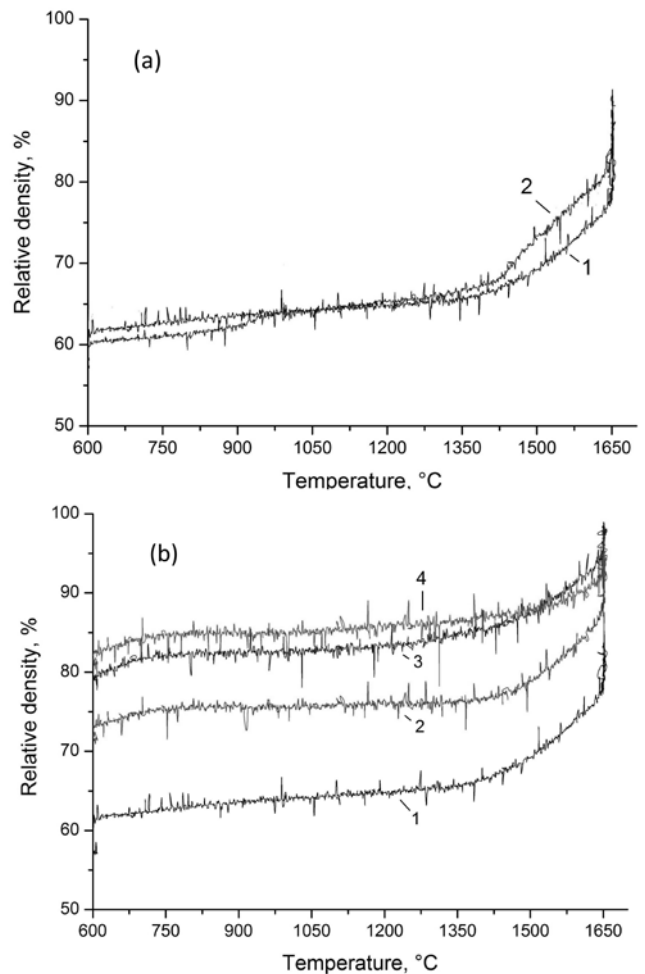


Fig. 4. Relative density  $\rho_{\text{rel}}$  as a function of temperature  $T$  for: (a)  $\beta$ - $\text{Si}_5\text{AlON}_7$  (1) and  $\beta$ - $\text{Si}_5\text{AlON}_7$ - $\text{Y}_2\text{O}_3$  (5 wt %) (2); and (b)  $\beta$ - $\text{Si}_5\text{AlON}_7$  (1),  $\beta$ - $\text{Si}_5\text{AlON}_7$ -BN (10 wt %) (2),  $\beta$ - $\text{Si}_5\text{AlON}_7$ -BN (20 wt %) (3), and  $\beta$ - $\text{Si}_5\text{AlON}_7$ -BN (30 wt %) (4);  $T_{\text{max}} = 1650^\circ\text{C}$ .

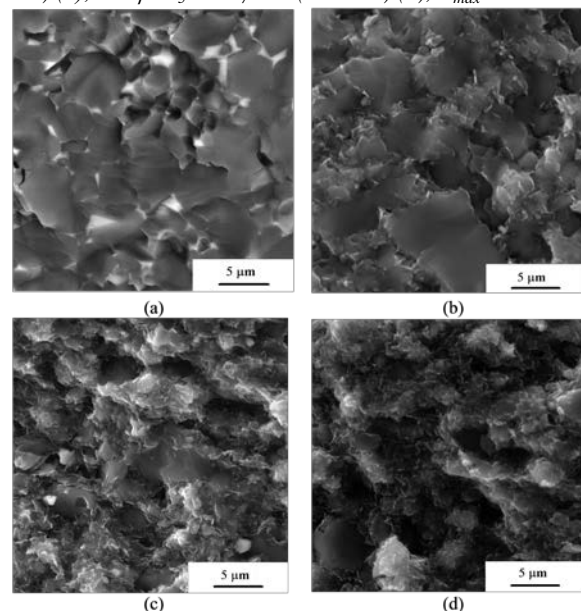
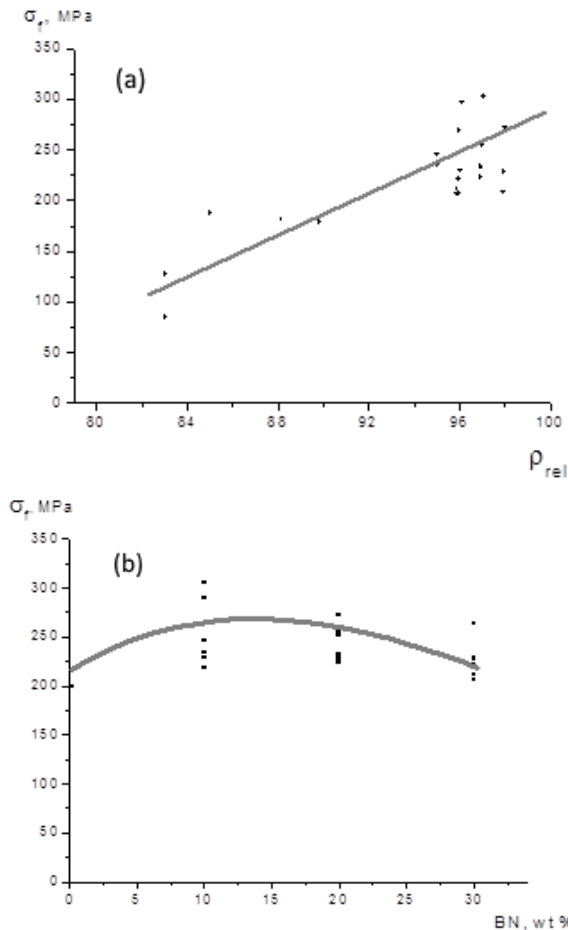


Fig. 5. Fracture surface of sintered ceramic composites: (a)  $\beta$ - $\text{Si}_5\text{AlON}_7$ - $\text{Y}_2\text{O}_3$  (5 wt %), (b)  $\beta$ - $\text{Si}_5\text{AlON}_7$ -BN (10 wt %), (c)  $\beta$ - $\text{Si}_5\text{AlON}_7$ -BN (20 wt %), and (d)  $\beta$ - $\text{Si}_5\text{AlON}_7$ -BN (30 wt %);  $T_{\text{max}} = 1750^\circ\text{C}$ .

As is seen in Figs. 5b–d, small flaky h-BN particles are uniformly distributed over the surface of larger  $\beta$ -Si<sub>3</sub>AlON<sub>7</sub> particulates. At BN = 30 wt %, the h-BN particles unwettable with oxide melts fully isolate  $\beta$ -Si<sub>3</sub>AlON<sub>7</sub> particles apart (Fig. 5d). It is clear that in such and similar systems the contribution from liquid-phase processes in consolidation cannot be important. In case of 10 and 20 wt % h-BN, the processes associated with formation of liquid eutectics are more or less pronounced, so that high relative density (close to theoretical one) can be attained even in the absence of Y<sub>2</sub>O<sub>3</sub>.



**Fig. 6.** Flexural strength  $\sigma_f$  as a function of: (a) relative density  $\rho_{rel}$  of  $\beta$ -Si<sub>3</sub>AlON<sub>7</sub>-BN ceramics and (b) their BN content ( $\rho_{rel} = 0.95$ – $0.98$ ).

Figure 6a illustrates flexural strength  $\sigma_f$  as a function of  $\rho_{rel}$  for  $\beta$ -Si<sub>3</sub>AlON<sub>7</sub>-BN ceramics. This parameter ( $\rho_{rel}$ ) is used as a measure for strength parameters of sintered ceramic composites. Our results well agree with those reported for similar ceramic composites prepared by other techniques [12–14]. SPS method affords to produce ceramic composites with higher relative density and flexural strength (250–300 MPa). In our case, the flexural strength of synthesized ceramics was found to depend on the BN content only slightly (Fig. 6b).

#### 4. Conclusions

High-density  $\beta$ -SiAlON-BN (0–30 wt %) ceramic composites with improved strength properties were prepared by spark plasma sintering of SHS-produced  $\beta$ -Si<sub>3</sub>AlON<sub>7</sub> and BN powders. Thus obtained machinable ceramics seem promising for fabrication of machine parts and items operating in severe conditions of strong thermal shock and corrosion-active media.

#### Acknowledgments

This work was financially supported by the Russian Foundation for Basic Research (project no. 15-03-01051-a) and the Russian Science Foundation (project no.16-19-10213).

#### References

1. Ekström, T., and Nygren, M., SiAlON ceramics, *J. Am. Ceram. Soc.*, 1992, vol. 75, no. 2, pp. 259–276.
2. Haubner, R., Wilhelm, M., Weissenbacher, R., and Lux, B., Boron nitrides: Properties, synthesis, and applications, *Struct. Bonding*, 2002, vol. 102, no. 1, pp. 1–45.
3. Shuba, R., and Chen, I.-W., Machinable  $\alpha$ -SiAlON/BN composites, *J. Am. Ceram. Soc.*, 2006, vol. 89, no. 7, pp. 2147–2153.
4. Wei, D., Meng, Q., and Jia, D., Mechanical and tribological properties of hot-pressed h-BN/Si<sub>3</sub>N<sub>4</sub> ceramic composites, *Ceram. Int.*, 2006, vol. 32, no. 5, pp. 549–554.
5. Gao, L., Jin, X., Li, J., Li, Y., and Sun, J., BN/Si<sub>3</sub>N<sub>4</sub> nanocomposite with high strength and good machinability, *Mater. Sci. Eng. A*, 2006, vol. 415, nos. 1–2, pp. 145–148.
6. Zhao, Y.S., Yang, Y., Li, J.T., Borovinskaya, I.P., and Smirnov, K.L., Temperature factor in tailoring the morphology of Y- $\alpha$ -SiAlON microcrystals fabricated by combustion synthesis, *Int. J. Self-Propag. High-Temp. Synth.*, 2009, vol. 18, no 2, pp. 87–91.
7. Fu, R., Chen, K.X., and Ferreira, J.M.F., Combustion synthesis of  $\beta$ -SiAlON whiskers, *Key Eng. Mater.*, 2005, vol. 280–283, pp. 1241–1244.
8. Niu, J., Yi, X., Nakatsugawa, I., and Akiyama, T., Salt-assisted combustion synthesis of  $\beta$ -SiAlON fine powders, *Intermetallics*, 2013, vol. 35, no. 1, pp. 53–59.
9. Munir, Z.A., Anselmi-Tamburini, U., Ohyanagi, M., The effect of electric field and pressure on the synthesis and consolidation of materials: A review of the spark plasma sintering method, *J. Mater. Sci.*, 2006, vol. 41, no 3, pp. 763–777.
10. Voisin, T., Durand, L., Karnatak, N., Le Gallet, S., Thomas, M., Le Berre, Y., Castagné, J.-F., and Couret, A., Temperature control during spark plasma sintering and application to up-scaling and complex shaping, *J. Mater. Process. Technol.*, 2013, vol. 213, no 2, pp. 269–278.
11. Loryan, V.E., Borovinskaya, I.P., Smirnov, K.L., and Titov, S.G., Sintering of SHS-produced  $\alpha$ -Si<sub>3</sub>N<sub>4</sub>,  $\alpha$ -SiAlON, and  $\beta$ -SiAlON, *Int. J. Self-Propag. High-Temp. Synth.*, 2012, vol. 21, no 1, pp. 41–44.
12. Smirnov, K.L., and Borovinskaya, I.P., Combustion synthesis of SiAlON-based ceramic composites, *Powder Metall. Met. Ceram.*, 2003, vol. 42, nos. 11–12, pp. 596–602.
13. Yuan, B., Liu, J.-X., Zhang, G.-J., Kan, Y.-M., and Wang, P.-L., Silicon nitride/boron nitride ceramic composites fabricated by reactive pressureless sintering, *Ceram. Int.*, 2009, vol. 35, no 6, pp. 2155–2159.
14. Zhang, G.-J., Yang, J.-F., Ando, M., and Ohji, T., SiAlON-boron nitride porous composites: In situ synthesis, microstructure, and properties, *Key Eng. Mater.*, 2003, vol. 237, pp. 123–128.